

Facile S–S Bond Activation of Alkyl and Aryl Disulfides by $[\text{RuCp}(\text{CH}_3\text{CN})_3]^+$: Formation of Dinuclear Ru(III)–Ru(III) Complexes with Bridging Thiolate Ligands[†]

Eva Becker,[‡] Kurt Mereiter,[§] Roland Schmid,[‡] and Karl Kirchner^{*;‡}

Institute of Applied Synthetic Chemistry and Institute of Chemical Technologies and Analytics, Vienna University of Technology, Getreidemarkt 9, A-1060 Vienna, Austria

Received February 13, 2004

We describe a way to enter into dinuclear RuCp thiolate chemistry, since hitherto only the RuCp* derivatives have been available. When the labile cationic complex $[\text{RuCp}(\text{CH}_3\text{CN})_3]^+$ is reacted with alkyl or aryl disulfides RSSR (and likewise PhSeSePh), oxidative addition takes place. As a result, dinuclear Ru(III)–Ru(III) complexes of the type $[\text{CpRu}(\text{CH}_3\text{CN})(\mu\text{-SR})_2(\text{CH}_3\text{CN})\text{RuCp}](\text{PF}_6)_2$ are formed, featuring a metal–metal single bond and bridging thiolate ligands. The reaction of $[\text{RuCp}(\text{CH}_3\text{CN})_3]^+$ with bis(2-pyridyl) disulfide affords, depending on the reaction conditions, either the dinuclear complex $[\text{CpRu}(\mu\text{-pyS})_2\text{RuCp}](\text{PF}_6)_2$ or the mononuclear complex $[\text{CpRu}(\kappa^2\text{N},\text{S-pyS})_2]\text{PF}_6$. The substitutionally labile acetonitrile ligands in $[\text{CpRu}(\text{CH}_3\text{CN})(\mu\text{-SR})_2(\text{CH}_3\text{CN})\text{RuCp}](\text{PF}_6)_2$ are readily replaced by other donor ligands. For instance, treatment of $[\text{CpRu}(\text{CH}_3\text{CN})(\mu\text{-S-}t\text{-Bu})_2(\text{CH}_3\text{CN})\text{RuCp}](\text{PF}_6)_2$ with KBr affords the neutral complex $\text{CpRuBr}(\mu\text{-S-}t\text{-Bu})_2\text{BrRuCp}$, while with *t*-BuSH the dinuclear complex *sym*- $[\text{CpRu}(\mu\text{-S-}t\text{-Bu})_3\text{RuCp}]\text{PF}_6$ containing three bridging thiolate ligands is formed. Representative X-ray structures are presented.

Introduction

Dinuclear RuCp* complexes containing bridging thiolate ligands are a well-established class of compounds. They not only exhibit unique reactivities toward many substrates such as alkynes, H₂, and CO,^{1–3} but also are active catalysts in various C–C and C–heteroatom bond-forming reactions. Examples are the propargylic alkylation of propargylic alcohols with ketones,⁴ substitution reactions of propargylic alcohols with thiols,⁵ and the cycloaddition of propargylic alcohols with phenol derivatives.⁶ The ruthenium complexes under consideration are commonly obtained by reacting the readily available precursors $[\text{RuCp}^*(\mu\text{-Cl})_4]$ and $\text{Cp}^*\text{RuCl}(\mu\text{-Cl})_2\text{RuCp}^*\text{Cl}$ with thiolates.¹ This methodology is restricted to the Cp* coligand, since the respective precursor complexes with parent Cp are unavailable. This

* To whom correspondence should be addressed. E-mail: kkirch@mail.zserv.tuwien.ac.at.

[†] Dedicated to Prof. Peter Stanetty on the occasion of his 60th birthday.

[‡] Institute of Applied Synthetic Chemistry.

[§] Institute of Chemical Technologies and Analytics.

(1) (a) Hidai, M.; Imagawa, K.; Cheng, G.; Mizobe, Y.; Wakatsuki, Y.; Yamazaki, H. *Chem. Lett.* **1986**, 1299. (b) Tanase, T.; Imagawa, K.; Dev, S.; Mizobe, Y.; Yano, S.; Hidai, M. *New J. Chem.* **1988**, 12, 697. (c) Dev, S.; Imagawa, K.; Mizobe, Y.; Cheng, G.; Wakatsuki, Y.; Yamazaki, H.; Hidai, M. *Organometallics* **1989**, 8, 1232. (d) Takahashi, A.; Mizobe, Y.; Hidai, M. *Chem. Lett.* **1994**, 371.

(2) Takahashi, A.; Mizobe, Y.; Matsuzaka, H.; Dev, S.; Hidai, M. *J. Organomet. Chem.* **1993**, 456, 243.

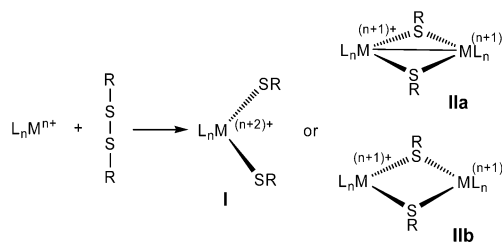
(3) Dev, S.; Mizobe, Y.; Hidai, M. *Inorg. Chem.* **1990**, 29, 4797.

(4) Nishibayashi, Y.; Wakiji, I.; Ishii, Y.; Uemura, S.; Hidai, M. *J. Am. Chem. Soc.* **2001**, 123, 3393.

(5) Inada, Y.; Nishibayashi, Y.; Hidai, M.; Uemura, S. *J. Am. Chem. Soc.* **2002**, 124, 15172.

(6) Nishibayashi, Y.; Inada, Y.; Hidai, M.; Uemura, S. *J. Am. Chem. Soc.* **2002**, 124, 7900.

Scheme 1



may simply be the reason thiolate-bridged complexes of the RuCp fragment have not been reported so far.

Alternatively, thiolate complexes may be generated by oxidative addition of alkyl and aryl disulfides to transition-metal complexes. The result may be either mononuclear bis(thiolate) (I) or dinuclear complexes with bridging thiolate ligands of types IIa and IIb according to Scheme 1.⁷

In the present paper, we will investigate the potential of the labile cationic complex $[\text{RuCp}(\text{CH}_3\text{CN})_3]^+$ toward the oxidative addition of alkyl and aryl disulfides as an entry into dinuclear RuCp thiolate chemistry.

(7) (a) Liaw, W.-F.; Hsieh, C.-H.; Peng, S.-M.; Lee, G.-H. *Inorg. Chim. Acta* **2002**, 332, 153. (b) Lee, C.-M.; Lin, G.-Y.; Hsieh, C.-H.; Hu, C.-H.; Lee, G.-H.; Peng, S.-M.; Liaw, W.-F. *J. Chem. Soc., Dalton Trans.* **1999**, 2393. (c) Liaw, W.-F.; Chen, C.-H.; Lee, G.-H.; Peng, S.-M. *Organometallics* **1998**, 17, 2370. (d) Lang, R. F.; Ju, T. D.; Kiss, G.; Hoff, C. D.; Bryan, J. C.; Kubas, G. J. *Inorg. Chem.* **1994**, 33, 3899. (e) Haines, R. J.; de Beer, J. A.; Greatrex, R. *J. Organomet. Chem.* **1975**, 85, 89. (f) Zanella, R.; Ros, R.; Graziani, M. *Inorg. Chem.* **1973**, 12, 2736. (g) Lam, C. T.; Senoff, C. V. *Can. J. Chem.* **1973**, 51, 3790. (h) Köpf, H.; Block, B. *Z. Naturforsch.* **1968**, 23b, 1536.

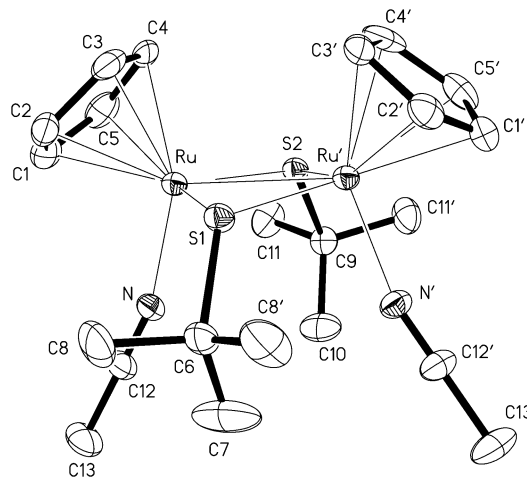


Figure 1. Structural view of $[CpRu(CH_3CN)(\mu\text{-}S\text{-}t\text{-}Bu)_2\text{-(}CH_3CN\text{)RuCp}](PF_6)_2$ (**2a**) showing 20% thermal ellipsoids (PF_6^- omitted for clarity). The complex is mirror symmetric, and primed atoms are symmetry equivalents of unprimed ones.

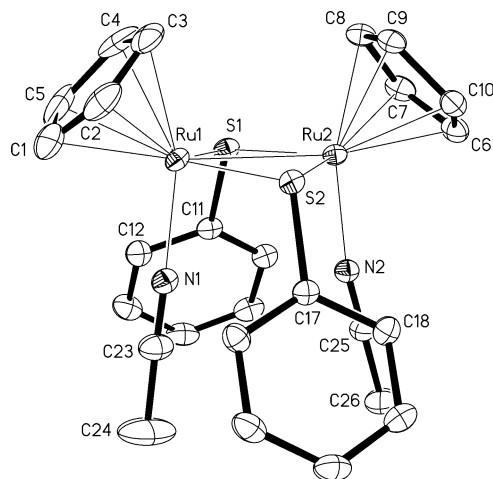
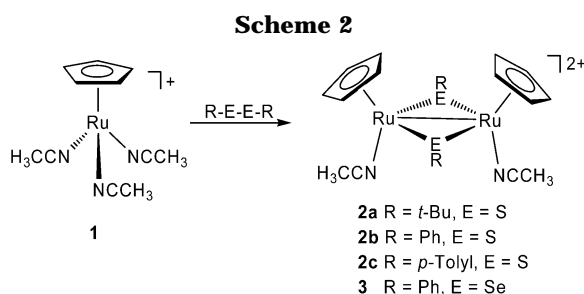


Figure 2. Structural view of $[CpRu(CH_3CN)(\mu\text{-}SPh)_2(CH_3CN)RuCp](PF_6)_2\cdot\text{solv}$ (**2b·solv**) showing 40% thermal ellipsoids (PF_6^- and solvent omitted for clarity).



Results and Discussion

Treatment of $[RuCp(CH_3CN)_3]PF_6$ (**1**) with 0.5 equiv of the disulfides RSSR (R = *t*-Bu, Ph, *p*-tolyl) at 50 °C results in the formation of the diruthenium complexes $[CpRu(CH_3CN)(\mu\text{-}SR)_2(CH_3CN)RuCp](PF_6)_2$ (**2a–c**) in essentially quantitative yields (Scheme 2). In a similar fashion, the reaction of **1** with PhSeSePh yields the selenolate analogue $[CpRu(CH_3CN)(\mu\text{-}SePh)_2(CH_3CN)RuCp](PF_6)_2$ (**3**) in 97% yield. All these complexes are air-stable both in solution and in the solid state. Characterization was accomplished by 1H and $^{13}C\{^1H\}$ NMR spectroscopy as well as elemental analysis. The 1H and $^{13}C\{^1H\}$ NMR spectra of **2a–c** exhibit sharp lines indicating their diamagnetic nature; i.e., the presence of a Ru–Ru single bond. Complexes **2a–c** give rise to only one set of Cp signals, whereas for **3** two Cp resonances are observed in a 3:1 ratio, suggesting the presence of isomeric complexes. The Cp ligand exhibits a singlet in the range 5.5–6.0 ppm. The proton resonance of the CH_3CN ligand gives a singlet in the range 1.6–1.8 ppm.

The solid-state structures of **2a, b** and **3** were determined by single-crystal X-ray diffraction, confirming their dinuclear nature. ORTEP plots are depicted in Figures 1–3, with selected bond distances and angles being reported in Table 1.

All complexes contain two $RuCp$ units in a mutually *cis* configuration bridged by two thiolate ligands and selenolate ligands, respectively, with the substituents adopting a *syn* orientation with respect to one another but *anti* with respect to the Cp ligands (it has to be

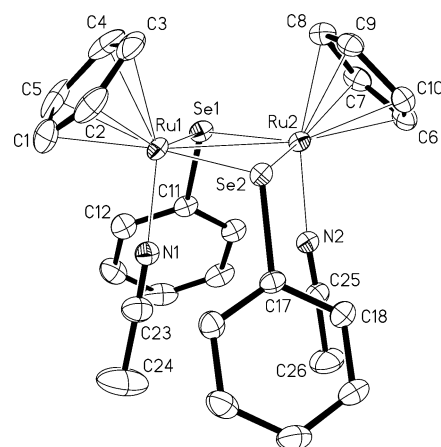
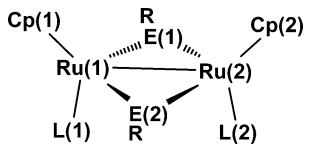


Figure 3. Structural view of $[CpRu(CH_3CN)(\mu\text{-}SePh)_2\text{-(}CH_3CN\text{)RuCp}](PF_6)_2\cdot\text{solv}$ (**3·solv**) showing 40% thermal ellipsoids (PF_6^- and solvent omitted for clarity).

noted that for **3** also another minor isomer crystallized with a mutual *anti* orientation of the two Ph substituents; see Cambridge Crystallographic Database structure CCDC-231190). The remaining coordination sites are occupied by two CH_3CN ligands. Similar structural features are observed also for the related thiolate-bridged $RuCp^*$ complexes.^{2,3,8} The Ru_2S_2 rings are puckered with deviations from the common least-squares planes of ± 0.089 Å for **2a** and ± 0.063 Å for **2b·solv**. Similar geometric features are observed for the Ru_2Se_2 core in **3·solv** (ring pucker ± 0.062 Å). The Ru–Ru distances of **2a, c** and **3** of 2.781(1), 2.753(1), and 2.819(1) Å, respectively, are indicative of a Ru–Ru single bond, consistent with a diamagnetic nature despite the formal oxidation state of +III. The Ru–S distances in the range 2.305–2.312 Å are comparable to those of other thiolate-bridged diruthenium centers with Ru(III) centers.^{2,3,8} Likewise, the Ru–Se bond distances of 2.419(1) and 2.424(1) Å are in the expected range.

In similar fashion, if **1** is treated with 0.5 equiv of bis(2-pyridyl) disulfide at room temperature, the di-

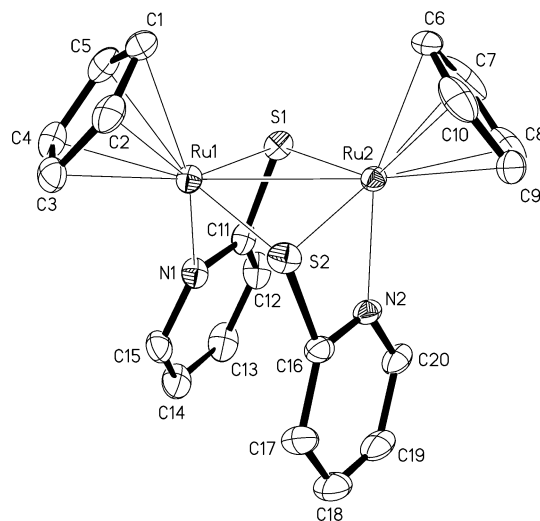
(8) (a) Nishio, M.; Matsuzaka, H.; Mizobe, Y.; Hidai, M. *Organometallics* **1996**, *15*, 965 and references therein. (b) Takagi, Y.; Matsuzaka, H.; Ishii, Y.; Hidai, M. *Organometallics* **1997**, *16*, 4445.

Table 1. Selected Bond Distances (Å) and Angles (deg) for **2a**, **2b**·solv, **3**·solv, **4**, and **6a**·solv


	2a	2b ·solv	3 ·solv	6a ·solv
E	S	S	Se	S
R	<i>t</i> -Bu	Ph	Ph	<i>t</i> -Bu
L	CH ₃ CN	CH ₃ CN	CH ₃ CN	Br
Ru(1)–Ru(2)	2.781(1)	2.753(1)	2.819(1)	2.802(1)
Ru(1)–Cp(1)	2.198(5)	2.203(3)	2.190(4)	2.224(5)
Ru(2)–Cp(2)	2.198(5)	2.210(3)	2.203(4)	2.224(5)
Ru(1)–E(1)	2.317(1)	2.309(1)	2.419(1)	2.306(1)
Ru(1)–E(2)	2.305(1)	2.312(1)	2.421(1)	2.312(1)
Ru(2)–E(1)	2.317(1)	2.311(1)	2.424(1)	2.312(1)
Ru(2)–E(2)	2.305(1)	2.308(1)	2.421(1)	2.306(1)
Ru(1)–L(1)	2.062(4)	2.049(2)	2.039(3)	2.559(1)
Ru(2)–L(2)	2.062(4)	2.045(2)	2.037(3)	2.559(1)
Ru(1)–E(1)–Ru(2)	73.8(1)	73.2(1)	71.2(1)	74.7(1)
Ru(1)–E(2)–Ru(2)	74.2(1)	73.1(1)	71.2(1)	74.7(1)
E(1)–Ru(1)–E(2)	105.3(1)	106.5(1)	108.6(1)	79.1(4)
E(1)–Ru(2)–E(2)	105.3(1)	106.5(1)	108.4(1)	79.1(4)

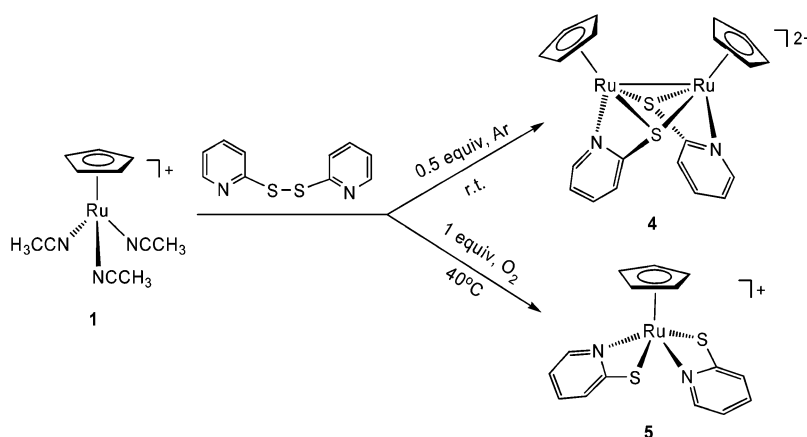
nuclear complex [CpRu(μ -pyS)₂RuCp](PF₆)₂ (**4**) is obtained in 93% isolated yield, as shown in Scheme 3. A series of NMR experiments implicate the formulation of diamagnetic species: in the ¹H NMR spectrum the hydrogen atoms of the Cp ring were shifted downfield to 6.14 ppm, reemphasizing a higher oxidation state of the ruthenium center. Similarly, in the ¹³C{¹H} NMR spectrum the ring carbon atoms of the Cp ligand were found to be shifted downfield, appearing as a singlet at 90.3 ppm. On the basis of these results and the diamagnetic nature of **4**, the Ru(II) metal center was apparently oxidized to Ru(III), forming binuclear species with a metal–metal bond. The X-ray structure analysis of **4** depicted in Figure 4 confirms the dimeric nature.

Selected bond distances and angles are reported in the caption. The Cp ligands are in a mutually cis configuration. The pyS ligand acts as both a κ^2N,S chelating ligand and a bridging ligand. The core of the dinuclear complex consists of a four-membered Ru₂S₂ ring with a ring pucker of ± 0.164 Å, which is distinctly larger than in **2a** and **2b**·solv. The S(1)–Ru(1)–S(2) and S(1)–Ru(2)–S(2) angles are 103.9(1) and 103.7(1)°, respectively. The Ru(1)–Ru(2) distance of 2.789(1) Å clearly indicates the presence of a metal–metal single

**Figure 4.** Structural view of [CpRu(μ -pyS)₂RuCp](PF₆)₂ (**4**) showing 20% thermal ellipsoids (PF₆[−] omitted for clarity). Selected bond lengths (Å) and angles (deg): Ru(1)–C(1–5)_{av} = 2.199(5), Ru(2)–C(6–10)_{av} = 2.183(6), Ru(1)–Ru(2) = 2.789(1), Ru(1)–N(1) = 2.103(4), Ru(1)–S(1) = 2.331(1), Ru(1)–S(2) = 2.311(1), Ru(2)–N(2) = 2.093(4), Ru(2)–S(1) = 2.309(1), Ru(2)–S(2) = 2.337(1); Ru(1)–S(1)–Ru(2) = 73.9(1), Ru(1)–S(2)–Ru(2) = 73.8(1), N(1)–Ru(1)–S(1) = 67.6(1), N(2)–Ru(2)–S(2) = 68.0(1), S(1)–Ru(1)–S(2) = 103.9(1), S(1)–Ru(2)–S(2) = 103.7(1).

bond.⁸ The two pyS ligands form four-membered RuNCS rings with S(1)–Ru(1)–N(1) and S(2)–Ru(2)–N(2) angles of 67.6(1) and 68.0(1)°, respectively.

On the other hand, if **1** is reacted with 1 equiv of bis-(2-pyridyl) disulfide at 40 °C in the presence of air, the formation of **4** is completely suppressed and instead the mononuclear complex [CpRu(κ^2N,S -pyS)₂]PF₆ (**5**) is formed in 74% isolated yield (Scheme 3) containing two κ^2N,S chelating pyS ligands. This complex is air-stable in solution and in the solid state. Characterization was accomplished by ¹H and ¹³C{¹H} NMR spectroscopy and elemental analysis, as well as X-ray crystallography. An ORTEP plot of **5** is shown in Figure 5, with selected bond distances and angles being given in the caption. Accordingly, **5** adopts a four-legged piano-stool conformation with the N and S atoms of the two pyS ligands as the legs. The two pyS ligands are coordinated in such a way that the N and S atoms are cis to one another. The bond lengths Ru–N(1), Ru–N(2), Ru–S(1), and Ru–S(2) are 2.086(1), 2.081(1), 2.405(1), and 2.396(1)

Scheme 3

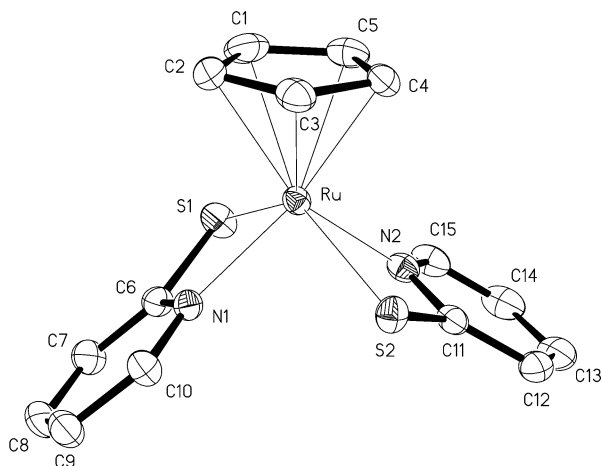
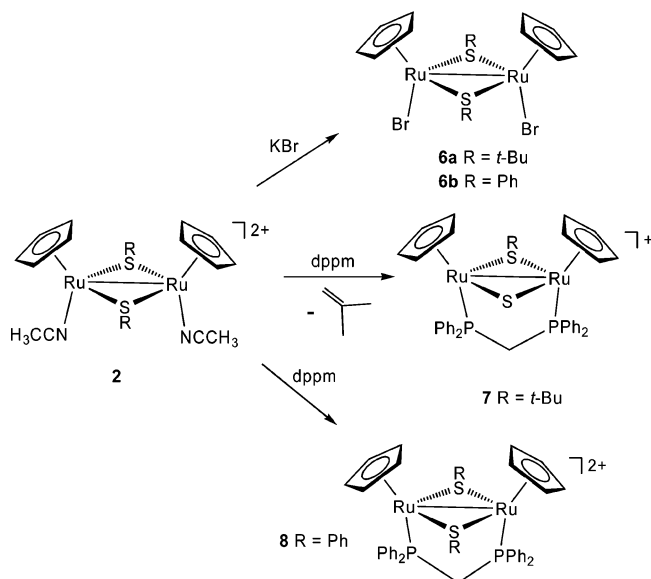


Figure 5. Structural view of [CpRu(κ^2 N,S-pyS)₂]PF₆ (**5**) showing 40% thermal ellipsoids (PF₆⁻ omitted for clarity). Selected bond lengths (Å) and angles (deg): Ru–C(1–5)_{av} = 2.222(2), Ru–S(1) = 2.405(1), Ru–S(2) = 2.396(1), Ru–N(1) = 2.086(1), Ru–N(2) = 2.081(1); N(1)–Ru–S(1) = 67.2(1), N(2)–Ru–S(2) = 67.0(1).

Scheme 4



Å, respectively. The two pyS ligands form four-membered-ring systems with S(1)–Ru–N(1) and S(2)–Ru–N(2) angles of 67.2(1) and 67.0(1)^o, respectively.

The substitutionally labile acetonitrile ligands in **2** are readily replaced by other donor ligands (Scheme 4). Thus, upon treatment of **2a,c** with KBr the neutral complexes CpRuBr(μ -S-*t*-Bu)₂BrRuCp (**6a**) and CpRuBr(μ -S-*p*-tolyl)₂BrRuCp (**6b**) become accessible. In a similar fashion **2a** and **2b** react with dppm to yield the complexes [CpRu(μ -dppm)(μ -S)(μ -S-*t*-Bu)RuCp]PF₆ (**7**) and [CpRu(μ -dppm)(μ -SPh)₂RuCp](PF₆)₂ (**8**). In the case of **2a**, the reaction is accompanied by loss of a *t*-Bu substituent of one of the two S-*t*-Bu ligands, converting it into a sulfido ligand and thereby releasing presumably isobutene (this has not been detected). All these complexes are air-stable solids. Characterization was afforded by elemental analysis and ¹H, ¹³C{¹H}, and ³¹P{¹H} NMR spectroscopy. **6a** and **7** have also been characterized by X-ray crystallography. Structural views are shown in Figures 6 and 7. Selected bond distances

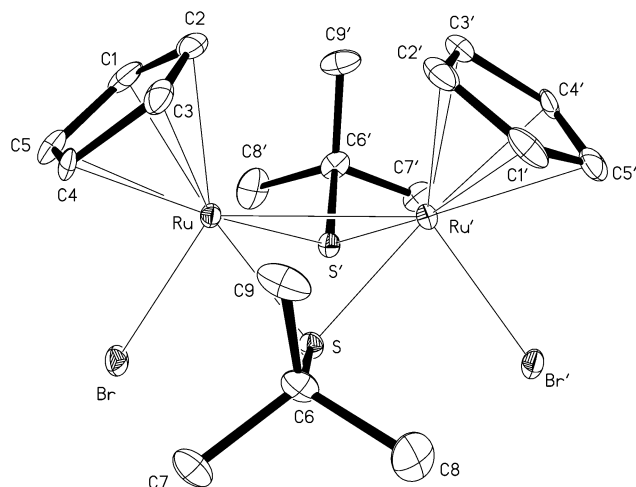


Figure 6. Structural view of [CpRuBr(μ -S-*t*-Bu)₂BrRuCp]·solv (**6a**·solv) showing 40% thermal ellipsoids (PF₆⁻ and solvent omitted for clarity).

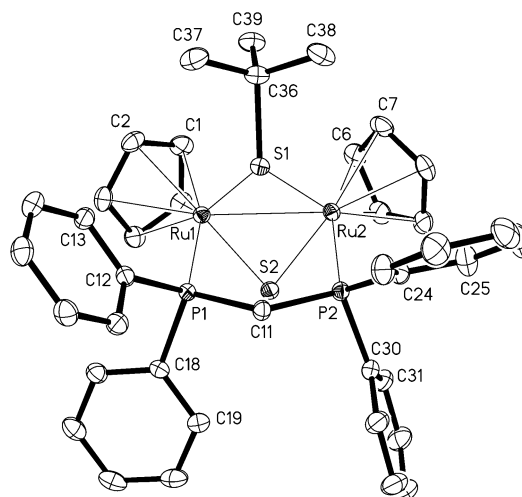


Figure 7. Structural view of [CpRu(μ -dppm)(μ -S)(μ -S-*t*-Bu)RuCp]PF₆·2(CH₃)₂CO (**7**·2(CH₃)₂CO) showing 40% thermal ellipsoids (PF₆⁻ and (CH₃)₂CO omitted for clarity). Selected bond lengths (Å) and angles (deg): Ru(1)–C(1–5)_{av} = 2.238(2), Ru(2)–C(6–10)_{av} = 2.241(2), Ru(1)–Ru(2) = 2.790(1), Ru(1)–P(1) = 2.292(1), Ru(1)–S(1) = 2.325(1), Ru(1)–S(2) = 2.305(1), Ru(2)–P(2) = 2.289(1), Ru(2)–S(1) = 2.331(1), Ru(2)–S(2) = 2.322(1); Ru(1)–S(1)–Ru(2) = 73.6(1), Ru(1)–S(2)–Ru(2) = 74.2(1).

and angles are summarized in Table 1 and in the caption.

Complex **6a** contains two RuCp units in a mutually cis configuration bridged by two thiolate ligands, with the substituents adopting a syn orientation with respect to one another. However, in contrast to **2**, the substituents are also syn oriented with respect to the Cp ligands. The remaining coordination sites are occupied by two Br⁻ ligands. The Ru–Ru' distance of 2.802(1) Å clearly indicates the presence of a metal–metal single bond. Similarly to **6a**, complex **7** contains two RuCp units in a mutually cis configuration bridged by one thiolate and one sulfido ligand. The remaining coordination sites are occupied by a bridging dppm ligand.

When **2a** was treated with *t*-BuSH (R = *t*-Bu, Ph) in nitromethane at 50 °C for 24 h, the symmetric dinuclear complex *sym*-[CpRu(μ -S-*t*-Bu)₃RuCp]PF₆ (**9a**) was obtained in 71% isolated yield (Scheme 5). Initially, the

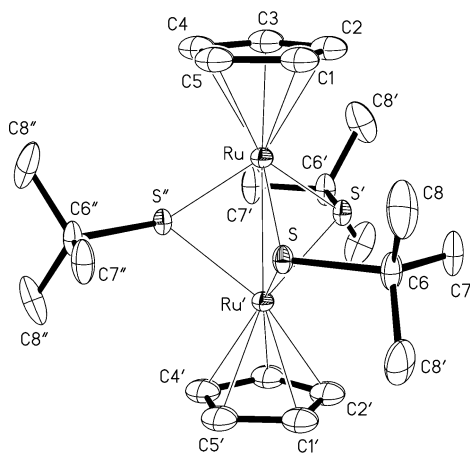
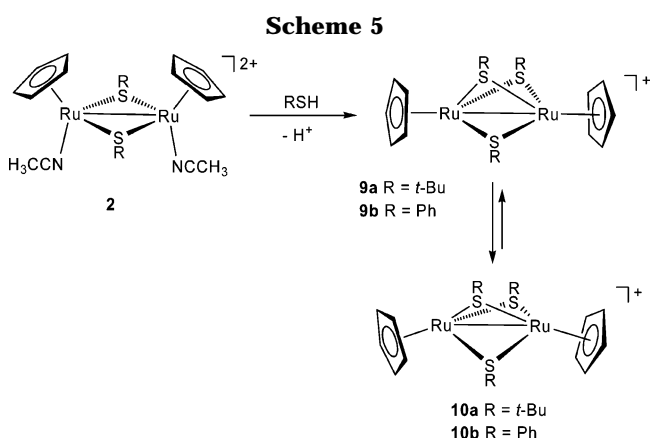


Figure 8. Structural view of *sym*-[CpRu(μ -S-*t*-Bu) $_3$ RuCp]-PF $_6$ (**9a**) showing 40% thermal ellipsoids (PF $_6^-$ omitted for clarity). Selected bond lengths (\AA) and angles (deg): Ru–C(1–5) $_{av}$ = 2.231(3), Ru–Ru = 2.638(1), Ru–S = 2.331(1); Ru–S–Ru = 68.9(1). Primed atoms are symmetry equivalents of unprimed ones.



solution NMR spectra of **9a** exhibited only one set of Cp and *t*-Bu resonances, in line with its highly symmetric structure, but after a few hours three individual signals for the *t*-Bu substituents appeared, while there is still only one set of Cp resonances present. This points to a slow isomerization into an asymmetric compound with the tentative formula *asym*-[CpRu(μ -S-*t*-Bu) $_3$ RuCp]-PF $_6$ (**10a**). The ratio of **9a** and **10a** could not be determined, due to partial precipitation of **9a** upon standing. Furthermore, attempts failed to isolate **10a** in pure form suitable for X-ray crystallography. A similar observation has been made upon treatment of **2b** with PhSH under the same reaction conditions, yielding an isomeric mixture of symmetrical and asymmetrical dinuclear complexes: viz., *sym*- and *asym*-[CpRu(μ -SPh) $_3$ RuCp]PF $_6$ (**9b**, **10b**). These complexes are present in an approximately 7:3 ratio. Also in this case, all attempts to separate the complexes proved unsuccessful.

The solid-state structure of **9a** was determined by single-crystal X-ray diffraction, confirming the dinuclear nature. An ORTEP diagram is depicted in Figure 8, with selected bond distances and angles being reported in the caption. The compound crystallizes in the hexagonal space group $P6_3/m$ and exhibits a C_{3h} symmetry for the dinuclear *sym*-[CpRu(μ -S-*t*-Bu) $_3$ RuCp] $^+$ complex, which is incompatible with the C_5 symmetry of the Cp rings. The resulting disorder of Cp was satisfactorily modeled

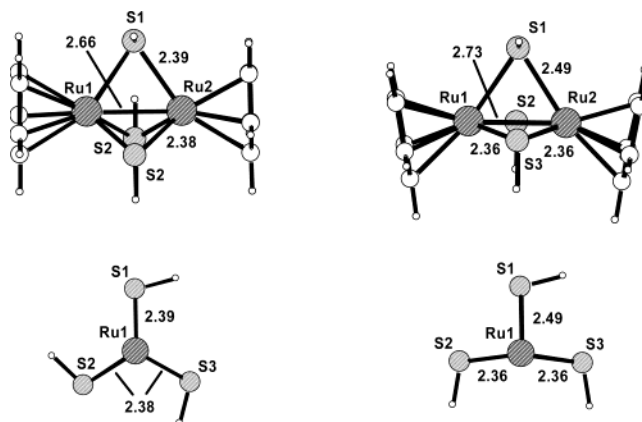


Figure 9. Optimized geometries for *sym*-[CpRu(μ -SH) $_3$ RuCp] $^+$ and *asym*-[CpRu(μ -SH) $_3$ RuCp] $^+$ calculated at the B3LYP (Ru sdd; C, H, S 6–31g **) level of theory (top) with a view along the Ru–Ru vector (bottom).

by introducing an idealized five-membered ring with occupancy $1/3$ in three symmetry-equivalent orientations, only one of which is shown in Figure 8. The Ru–Ru bond length of 2.638(1) \AA is close to that in the related RuCp * complex *sym*-[Cp * Ru(μ -SPh) $_3$ RuCp *] $^+$ (2.630(1) \AA). 3

In the absence of structural data for the asymmetric complexes **10a**, **b**, we performed DFT/B3LYP calculations based on [CpRu(μ -SH) $_3$ RuCp] $^+$ used as a model to obtain some structural hints. We were in fact able to locate a stationary point for *asym*-[CpRu(μ -SH) $_3$ RuCp] $^+$, which is 1.4 kcal/mol slightly more stable than the symmetric species (Figure 9). In *asym*-[CpRu(μ -SH) $_3$ RuCp] $^+$ the Cp rings are no longer parallel to one another. Furthermore, there are two sets of thiolate ligands featuring two short and one long Ru–S bond of 2.35 and 2.49 \AA , respectively. Also, the Ru–Ru bond distance of 2.73 \AA is slightly longer as compared to the symmetric complex. These results are fully consistent with the experimental NMR data involving a slow isomerization process.

The reliability of the computational method was checked by the calculations of the symmetric complex **9a**, using *sym*-[CpRu(μ -SH) $_3$ RuCp] $^+$ as a model. As a result, the DFT-optimized structure of the latter is in excellent agreement with the X-ray structure of **9a**, despite the absence of substituents (Figure 9).

Experimental Section

General Information. Manipulations were performed under an inert atmosphere of purified argon by using Schlenk techniques and/or a glovebox. All chemicals were standard reagent grade and were used without further purification. The solvents were purified according to standard procedures. 9 The deuterated solvents were purchased from Eurisotop and dried over 4 \AA molecular sieves. [RuCp(CH $_3$ CN) $_3$]PF $_6$ (**1**) was prepared according to the literature, 10 ^1H , $^{13}\text{C}\{^1\text{H}\}$, and $^{31}\text{P}\{^1\text{H}\}$ NMR spectra were recorded on a Bruker AC-250 spectrometer operating at 250.13, 62.86, and 101.26 MHz, respectively, and were referenced to SiMe $_4$ and H $_3$ PO $_4$ (85%).

Synthesis. [CpRu(CH $_3$ CN)(μ -S-*t*-Bu) $_2$ (CH $_3$ CN)RuCp]-PF $_6$ (**2a**). To a solution of **1** (100 mg, 0.230 mmol) in acetone (5 mL) was added *t*-BuSS-*t*-Bu (26.7 μL , 0.138 mmol), and the

(9) Perrin, D. D.; Armarego, W. L. F. *Purification of Laboratory Chemicals*, 3rd ed.; Pergamon: New York, 1988.

(10) Gill, T. P.; Mann, K. R. *Organometallics* **1982**, *1*, 485.

mixture was stirred for 24 h at 50 °C. After removal of the solvent a brown powder was obtained, which was collected on a glass frit, washed with Et₂O (3 × 5 mL), and dried under vacuum. Yield: 99 mg (98%). Anal. Calcd for C₂₂H₃₄F₁₂N₂P₂-Ru₂S₂: C, 29.94; H, 3.88; N, 3.17. Found: C, 29.88; H, 3.69; N, 3.20. ¹H NMR (δ, CD₃NO₂, 20 °C): 5.56 (s, 10H, Cp), 2.36 (s, 6H, CH₃), 1.66 (s, 18H, CH₃). ¹³C{¹H} NMR (δ, CD₃NO₂, 20 °C): 126.3 (NC), 89.4 (Cp), 60.2 (C(CH₃)₃), 33.1 (CH₃), 2.8 (NCCH₃).

[CpRu(CH₃CN)(μ-SPh)₂(CH₃CN)RuCp](PF₆)₂ (2b). This complex was prepared analogously to **2a** with **1** (100 mg, 0.230 mmol) and PhSSPh (30 mg, 0.138 mmol) as the starting materials. Yield: 103 mg (97%). Anal. Calcd for C₂₆H₂₆F₁₂N₂P₂-Ru₂S₂: C, 33.85; H, 2.84; N, 3.04. Found: C, 33.89; H, 2.91; N, 3.10. ¹H NMR (δ, CD₃NO₂, 20 °C): 7.47–7.24 (m, 10H, Ph), 5.99 (s, 10H, Cp), 1.36 (s, 6H, CH₃). ¹³C{¹H} NMR (δ, CD₃NO₂, 20 °C): 133.3 (Ph¹), 131.2 (NCCH₃), 131.0 (Ph^{2,6}), 129.0 (Ph⁴), 128.8 (Ph^{3,5}), 88.4 (Cp), 1.5 (NCCH₃).

[CpRu(CH₃CN)(μ-S-p-Tolyl)₂(CH₃CN)RuCp](PF₆)₂ (2c). This complex was prepared analogously to **2a** with **1** (400 mg, 0.921 mmol) and (*p*-tolyl)SS(*p*-tolyl) (152 mg, 0.553 mmol) as the starting materials. Yield: 425 mg (97%). Anal. Calcd for C₂₈H₃₀F₁₂N₂P₂Ru₂S₂: C, 35.37; H, 3.18; N, 2.95. Found: C, 35.41; H, 3.21; N, 3.03. ¹H NMR (δ, CD₃NO₂, 20 °C): 7.30–7.15 (m, 8H, *p*-tolyl), 5.94 (s, 10H, Cp), 2.25 (s, 6H, CH₃), 1.36 (s, 6H, CH₃CN). ¹³C{¹H} NMR (δ, CD₃NO₂, 20 °C): 140.0 (*p*-tolyl¹), 131.0 (NCCH₃), 130.7 (*p*-tolyl^{2,6}), 129.9 (*p*-tolyl⁴), 129.5 (*p*-tolyl^{3,5}), 88.2 (Cp), 19.7 (CH₃), 1.6 (NCCH₃).

[CpRu(CH₃CN)(μ-SePh)₂(CH₃CN)RuCp](PF₆)₂ (3). This complex was prepared analogously to **2a** with **1** (100 mg, 0.230 mmol) and PhSeSePh (43 mg, 0.138 mmol) as the starting materials. In solution two isomers are present in an approximately 3:1 ratio. Yield: 113 mg (97%). Anal. Calcd for C₂₆H₂₆F₁₂N₂P₂Ru₂Se₂: C, 30.72; H, 2.58; N, 2.76. Found: C, 30.79; H, 2.63; N, 2.65. ¹H NMR (δ, CD₃NO₂, 20 °C): isomer **a**, 7.67–7.25 (m, 10H, Ph), 5.86 (s, 10H, Cp), 1.29 (s, 6H, CH₃); isomer **b**, 7.67–7.25 (m, 10H, Ph), 5.63 (s, 10H, Cp), 1.85 (s, 6H, CH₃).

[CpRu(μ-pyS)₂RuCp](PF₆)₂ (4). A solution of **1** (100 mg, 0.230 mmol) and bis(2-pyridyl) disulfide (pySSpy; 26 mg, 0.120 mmol) in nitromethane (5 mL) was stirred for 24 h at room temperature. The volume of the solution was then reduced to about 2 mL. By gas diffusion of Et₂O into this solution, dark green crystals were obtained, which were collected on a glass frit, washed with Et₂O (3 × 5 mL), and dried under vacuum. Yield: 90 mg (93%). Anal. Calcd for C₂₀H₁₈F₁₂N₂P₂Ru₂S₂: C, 28.51; H, 2.15; N, 3.32. Found: C, 28.65; H, 2.19; N, 3.40. ¹H NMR (δ, acetone-*d*₆, 20 °C): 7.74 (ddd, *J*_{HH} = 5.4 Hz, *J*_{HH} = 1.5 Hz, *J*_{HH} = 0.8 Hz, 2H, py⁶), 7.69 (dt, *J*_{HH} = 7.9 Hz, *J*_{HH} = 1.5 Hz, 2H, py⁴), 7.10 (ddd, *J*_{HH} = 8.1 Hz, *J*_{HH} = 1.3 Hz, *J*_{HH} = 0.8 Hz, 2H, py³), 6.89 (ddd, *J*_{HH} = 7.9 Hz, *J*_{HH} = 5.4 Hz, *J*_{HH} = 1.3 Hz, 2H, py⁵), 6.14 (s, 10H, Cp). ¹³C{¹H} NMR (δ, acetone-*d*₆, 20 °C): 165.2 (py²), 155.4 (py⁶), 139.9 (py⁴), 129.2 (py³), 124.8 (py⁵), 90.3 (Cp).

[CpRu(κ²N,S-pyS)₂PF₆ (5). A solution of **1** (100 mg, 0.230 mmol) and pySSpy (53 mg, 0.242 mmol, 1.05 equiv) in nitromethane (10 mL) was stirred for 4 h at 40 °C in the presence of air. The volume of the solution was then reduced to about 5 mL. By gas diffusion of Et₂O into this solution, red crystals were obtained which were collected on a glass frit, washed with Et₂O (3 × 5 mL), and dried under vacuum. Yield: 90 mg (74%). Anal. Calcd for C₁₅H₁₃F₆N₂PRuS₂: C, 33.90; H, 2.47; N, 5.27. Found: C, 33.78; H, 2.35; N, 5.24. ¹H NMR (δ, acetone-*d*₆, 20 °C): 8.58 (ddd, *J*_{HH} = 5.5 Hz, *J*_{HH} = 1.3 Hz, *J*_{HH} = 0.9 Hz, 2H, py⁶), 7.77 (tt, *J*_{HH} = 7.9 Hz, *J*_{HH} = 1.7 Hz, 2H, py⁴), 7.09 (ddd, *J*_{HH} = 7.4 Hz, *J*_{HH} = 5.5 Hz, *J*_{HH} = 1.3 Hz, 2H, py³), 7.03 (dt, *J*_{HH} = 8.5 Hz, *J*_{HH} = 0.9 Hz, 2H, py⁵), 6.39 (s, 5H, Cp). ¹³C{¹H} NMR (δ, acetone-*d*₆, 20 °C): 176.5 (py²), 153.1 (py⁶), 138.6 (py⁴), 126.5 (py³), 119.2 (py⁵), 95.2 (Cp).

[CpRuBr(μ-S-*t*-Bu)₂BrRuCp] (6a). To a solution of **2a** (100 mg, 0.113 mmol) in nitromethane (10 mL) was added KBr (100 mg, 0.840 mmol, 7.5 equiv), and the mixture was stirred for 24 h at room temperature. The reaction mixture was evaporated to dryness and the residue redissolved in CH₂Cl₂ (10 mL). Insoluble materials were removed by filtration. By gas diffusion of Et₂O into this solution, brown crystals were obtained, which were collected on a glass frit, washed with Et₂O (3 × 5 mL), and dried under vacuum. Yield: 45 mg (59%). Anal. Calcd for C₁₈H₂₈Br₂Ru₂S₂: C, 32.24; H, 4.21. Found: C, 32.33; H, 4.19. ¹H NMR (δ, CD₃NO₂, 20 °C): 5.48 (s, 10H, Cp), 1.42 (s, 18H, CH₃). ¹³C{¹H} NMR (δ, CD₃NO₂, 20 °C): 88.0 (Cp), 54.4 (C(CH₃)₃), 31.8 (CH₃).

[CpRuBr(μ-S-*p*-tolyl)₂BrRuCp] (6b). This complex was prepared analogously to **6a** with **2c** (100 mg, 0.105 mmol) and KBr (100 mg, 0.840 mmol) as the starting materials. Yield: 57 mg (72%). Anal. Calcd for C₂₄H₂₄Br₂Ru₂S₂: C, 39.03; H, 3.28. Found: C, 39.14; H, 3.11. ¹H NMR (δ, CD₂Cl₂, 20 °C): 7.35 (d, *J*_{HH} = 8.4 Hz, 4H, *p*-tolyl), 7.29 (d, *J*_{HH} = 8.4 Hz, 4H, *p*-tolyl), 5.03 (s, 10H, Cp), 2.41 (s, 6H, CH₃). ¹³C{¹H} NMR (δ, CD₂Cl₂, 20 °C): 142.9 (*p*-tolyl¹), 142.4 (*p*-tolyl⁴), 131.5 (*p*-tolyl^{2,6}), 130.4 (*p*-tolyl^{3,5}), 82.8 (Cp), 21.1 (CH₃).

[CpRu(μ-dppm)(μ-S)(μ-S-*t*-Bu)RuCp]PF₆ (7). A solution of **2a** (100 mg, 0.113 mmol) and dppm (48 mg, 0.124 mmol) in nitromethane (5 mL) was stirred for 24 h at room temperature. After reduction of the volume of the solution to about 2 mL, addition of Et₂O afforded a red-brown precipitate which was collected on a glass frit, washed with Et₂O (3 × 5 mL), and dried under vacuum. Yield: 108 mg (97%). Anal. Calcd for C₃₉H₄₁F₆P₃Ru₂S₂: C, 47.66; H, 4.20. Found: C, 47.76; H, 4.12. ¹H NMR (δ, CD₃NO₂, 20 °C): 7.72–7.20 (m, 20H, Ph), 5.55 (s, 10H, Cp), 2.75–2.48 (m, 2H, CH₂), 1.52 (s, 9H, CH₃). ¹³C{¹H} NMR (δ, CD₃NO₂, 20 °C): 139.6–127.8 (24C, Ph), 87.4 (Cp), 79.8 (t, *J*_{PF} = 1.9 Hz, CH₂), 56.4 (C(CH₃)₃), 32.4 (CH₃). ³¹P{¹H} NMR (δ, CD₃NO₂, 20 °C): 44.7 (PPh₂), –144.1 (*J*_{PF} = 708.4 Hz, PF₆).

[CpRu(μ-dppm)(μ-SPh)₂RuCp](PF₆)₂ (8). This complex was prepared analogously to **7** with **2b** (100 mg, 0.108 mmol) and dppm (46 mg, 0.119 mmol) as the starting materials. Yield: 129 mg (98%). Anal. Calcd for C₄₇H₄₂F₁₂P₄Ru₂S₂: C, 46.08; H, 3.46. Found: C, 46.11; H, 3.38. ¹H NMR (δ, CD₃NO₂, 20 °C): 7.88–7.24 (m, 30H, Ph), 5.23 (s, 10H, Cp), 3.22 (t, *J*_{HP} = 11.3 Hz, 2H, CH₂). ¹³C{¹H} NMR (δ, CD₃NO₂, 20 °C): 144.4–128.3 (Ph), 95.1 (Cp), 16.0 (t, *J*_{PF} = 23.1 Hz, CH₂). ³¹P{¹H} NMR (δ, CD₃NO₂, 20 °C): 36.6 (PPh₂), –144.7 (*J*_{PF} = 719.5 Hz, PF₆).

sym-[CpRu(μ-S-*t*-Bu)₃RuCp]PF₆ (9a) and asym-[CpRu(μ-S-*t*-Bu)₃RuCp]PF₆ (10a). A solution of **2a** (100 mg, 0.113 mmol) and *t*-BuSH (15.4 μL, 0.136 mmol) in nitromethane (5 mL) was stirred for 24 h at 50 °C. The volume of the solution was then reduced to about 2 mL. By gas diffusion of Et₂O into this solution, brown crystals were obtained, which were collected on a glass frit, washed with Et₂O (3 × 5 mL), and dried under vacuum. Yield: 60 mg (71%). Anal. Calcd for C₂₂H₃₇F₆PRu₂S₃: C, 35.48; H, 5.01. Found: C, 35.46; H, 5.10. ¹H NMR (δ, CD₃NO₂, 20 °C): 5.76 (s, 10H, Cp), 1.29 (s, 27H, CH₃). ¹³C{¹H} NMR (δ, CD₃NO₂, 20 °C): 81.6 (Cp), 53.4 (C(CH₃)₃), 29.4 (CH₃). In solution this complex slowly isomerized to partially afford the asymmetric complex **10a**, which could not be isolated in pure form. ¹H NMR (δ, CD₃NO₂, 20 °C): 5.66 (s, 10H, Cp), 1.41 (s, 9H, CH₃), 1.37 (s, 9H, CH₃), 1.04 (s, 9H, CH₃). ¹³C{¹H} NMR (δ, CD₃NO₂, 20 °C): 81.3 (Cp), 33.5 (CH₃), 28.7 (CH₃), 28.5 (CH₃); the quaternary carbon atoms of the *t*-Bu moiety were not observed.

sym-[CpRu(μ-SPh)₃RuCp]PF₆ (9b) and asym-[CpRu(μ-SPh)₃RuCp]PF₆ (10b). These complexes were prepared analogously to **9a** with **2b** (100 mg, 0.108 mmol) and thiophenol (13.4 μL, 0.130 mmol) as the starting materials. In solution the isomers **9b** and **10b** are present in an approximately 7:3 ratio. Overall yield: 73 mg (90.7%). Anal. Calcd for C₂₈H₂₅F₆-PRu₂S₃: C, 41.79; H, 3.85. Found: C, 42.04; H, 3.93. ¹H NMR

Table 2. Details for the Crystal Structure Determinations of Complexes 2a, 2b·solv, 3·solv, 4, 5, 6a·solv, 7·2(CH₃)₂CO, and 9a

	2a	2b·solv	3·solv	4	5	6a·solv	7·2(CH₃)₂CO	9a
formula	C ₂₂ H ₃₄ F ₁₂ N ₂ P ₂ Ru ₂ S ₂	C ₂₆ H ₂₆ F ₁₂ N ₂ P ₂ Ru ₂ S ₂	C ₂₆ H ₂₆ F ₁₂ N ₂ P ₂ Ru ₂ Se ₂	C ₂₀ H ₁₈ F ₁₂ N ₂ P ₂ Ru ₂ S ₂	C ₁₅ H ₁₃ F ₆ N ₂ PRuS ₂	C ₁₈ H ₂₈ Br ₂ Ru ₂ S ₂	C ₄₅ H ₅₃ F ₆ O ₂ P ₃ Ru ₂ S ₂	C ₂₂ H ₃₇ F ₆ P-Ru ₂ S ₃
fw	882.71	922.69	1016.49	842.56	531.43	670.48	1099.04	744.81
cryst size, mm	0.40 × 0.20 × 0.10	0.80 × 0.42 × 0.33	0.60 × 0.35 × 0.30	0.50 × 0.40 × 0.04	0.45 × 0.25 × 0.17	0.40 × 0.20 × 0.15	0.62 × 0.46 × 0.32	0.50 × 0.40 × 0.34
space group (No.)	<i>C2/m</i> (12)	<i>P2₁/n</i> (14)	<i>P2₁/n</i> (14)	<i>P2₁/c</i> (14)	<i>P2₁/n</i> (14)	<i>Pccn</i> (56)	<i>P1</i> (2)	<i>P6₃/m</i> (176)
<i>a</i> , Å	18.059(3)	12.821(1)	12.795(1)	10.619(3)	10.9202(6)	16.422(2)	13.198(3)	9.837(1)
<i>b</i> , Å	11.458(2)	23.404(1)	23.949(2)	17.964(5)	12.6724(6)	13.2400(18)	13.821(3)	9.837(1)
<i>c</i> , Å	17.789(3)	12.999(1)	13.028(1)	14.408(4)	13.6300(7)	13.4443(18)	14.347(4)	16.029(4)
α, deg	90	90	90	90	90	90	112.85(1)	90
β, deg	115.86(1)	108.287(1)	107.436(2)	100.74(1)	104.500(1)	90	91.94(1)	90
γ, deg	90	90	90	90	90	90	104.15(2)	120
<i>V</i> , Å ³	3312.3(10)	3703.3(3)	3808.7(4)	2700(1)	1826.1(2)	2923.1(7)	2314.1(10)	1343.4(4)
<i>Z</i>	4	4	4	4	4	4	2	2
ρ _{calcd} , g cm ⁻³	1.770	1.655	1.773	2.073	1.933	1.524	1.577	1.841
<i>T</i> , K	297(2)	173(2)	173(2)	297(2)	173(2)	100(2)	173(2)	173(2)
μ(Mo Kα), mm ⁻¹	1.219	1.095	2.866	1.491	1.236	3.909	0.907	1.470
<i>F</i> (000)	1752	1816	1960	1640	1048	1304	1116	748
abs cor	multiscan	multiscan	multiscan	multiscan	multiscan	multiscan	multiscan	multiscan
θ _{max} , deg	27	30	27	30	30	28.4	30	28.3
no. of rflns measd	19 993	54 553	45 906	32 582	25 236	19 615	55 383	15 355
no. of unique rflns	3792	10 705	8289	7756	5297	3522	13 331	1150
no. of rflns <i>I</i> > 2σ(<i>I</i>)	2908	9489	7260	5811	4922	3287	11639	1049
no. of params	220	417	417	377	244	109	546	95
R1 (<i>I</i> > 2σ(<i>I</i>)) ^a	0.0393	0.0367	0.0373	0.0443	0.0311	0.0426	0.0241	0.0211
R1 (all data)	0.0564	0.0423	0.0421	0.0656	0.0341	0.0451	0.0306	0.0244
wR2 (all data)	0.1214	0.0923	0.0974	0.1239	0.0777	0.1003	0.0621	0.0474
diff Fourier peaks	-0.56/0.74	-0.75/1.33	-0.85/1.64	-0.89/1.12	-0.39/1.08	-1.68/1.12	-0.52/0.83	-0.65/0.52
min/max, e Å ⁻³								

^a R1 = Σ||*F*_o| - |*F*_c||/Σ|*F*_o|; wR2 = [Σ(*wF*_o² - *F*_c²)/Σ(*wF*_o²)]^{1/2}.

(δ , CD₃NO₂, 20 °C): 7.70–7.05 (m, 15H, Ph), 5.65, 5.41 (2s, 10H, Cp). ¹³C{¹H} NMR (δ , CD₃NO₂, 20 °C): 145.2, 143.4 138.7 (Ph), 135.3–127.0 (Ph), 85.7 (Cp), 85.4 (Cp).

X-ray Structure Determination for 2a, 2b·solv, 3·solv, 4, 5, 6a·solv, 7·2(CH₃)₂CO, and 9a. Crystals of these complexes were obtained by diffusion of Et₂O into CH₃NO₂ or acetone solutions. Crystal data and experimental details are given in Table 2. X-ray data were collected on a Bruker Smart CCD area detector diffractometer using graphite-monochromated Mo K α radiation ($\lambda = 0.71073$ Å) and 0.3° ω -scan frames covering complete spheres of the reciprocal space. Corrections for absorption, $\lambda/2$ effects, and crystal decay were applied.¹¹ The structures were solved by direct methods using the program SHELXS97.¹² Structure refinement on F^2 was carried out with the program SHELXL97.¹² All non-hydrogen atoms were refined anisotropically. Hydrogen atoms were inserted in idealized positions and were refined riding with the atoms to which they were bonded, using AFIX 137 orientation refinement for acetonitrile CH₃ groups. In case of 2b·solv, 3·solv, and 6a·solv the disordered solvents (diethyl ether, nitromethane) were squeezed with the program PLATON prior to final refinement.¹³ The sulfide 2b·solv and selenide 3·solv are isostructural.

Computational Details. All calculations were performed using the Gaussian98 software package on the Silicon Graphics Origin 2000 of the Vienna University of Technology.¹⁴ The geometries and energies of the model complexes were optimized at the B3LYP level¹⁵ with the Stuttgart/Dresden ECP (SDD) basis set¹⁶ to describe the electrons of the Ru atom. For the H, C, and S atoms the 6-31g** basis set was employed.¹⁷ A vibrational analysis was performed to confirm that the

(11) Bruker programs: SMART, version 5.054; SAINT, version 6.2.9; SADABS, version 2.03; XPREP, version 5.1; SHELXTL, version 5.1 (Bruker AXS Inc., Madison, WI, 2001).

(12) Sheldrick, G. M. SHELX97: Program System for Crystal Structure Determination; University of Göttingen, Göttingen, Germany, 1997.

(13) Spek, A. L. PLATON: A Multipurpose Crystallographic Tool; University of Utrecht, Utrecht, The Netherlands, 2003.

structures of the model compounds have no imaginary frequency. The geometries were optimized without constraints (C_1 symmetry).

Acknowledgment. Financial support by the “Fonds zur Förderung der wissenschaftlichen Forschung” (Project No. P16600-N11) is gratefully acknowledged.

Supporting Information Available: Listings of atomic coordinates, anisotropic temperature factors, and all bond lengths and angles for complexes 2a, 2b·solv, 3·solv, 4, 5, 6a·solv, 7·2(CH₃)₂CO, and 9a; crystallographic data are also available as CIF files. This material is available free of charge via the Internet at <http://pubs.acs.org>.

OM0498854

(14) Frisch, M. J.; Trucks, G. W.; Schlegel, H. B.; Scuseria, G. E.; Robb, M. A.; Cheeseman, J. R.; Zakrzewski, V. G.; Montgomery, J. A., Jr.; Stratmann, R. E.; Burant, J. C.; Dapprich, S.; Millam, J. M.; Daniels, A. D.; Kudin, K. N.; Strain, M. C.; Farkas, O.; Tomasi, J.; Barone, V.; Cossi, M.; Cammi, R.; Mennucci, B.; Pomelli, C.; Adamo, C.; Clifford, S.; Ochterski, J.; Petersson, G. A.; Ayala, P. Y.; Cui, Q.; Morokuma, K.; Malick, D. K.; Rabuck, A. D.; Raghavachari, K.; Foresman, J. B.; Cioslowski, J.; Ortiz, J. V.; Stefanov, B. B.; Liu, G.; Liashenko, A.; Piskorz, P.; Komaromi, I.; Gomperts, R.; Martin, R. L.; Fox, D. J.; Keith, T.; Al-Laham, M. A.; Peng, C. Y.; Nanayakkara, A.; Gonzalez, C.; Challacombe, M.; Gill, P. M. W.; Johnson, B. G.; Chen, W.; Wong, M. W.; Andres, J. L.; Head-Gordon, M.; Replogle, E. S.; Pople, J. A. *Gaussian 98*, revision A.7; Gaussian, Inc.: Pittsburgh, PA, 1998.

(15) (a) Becke, A. D. *J. Chem. Phys.* **1993**, *98*, 5648. Miehlich, B.; Savin, A.; Stoll, H.; Preuss, H. *Chem. Phys. Lett.* **1989**, *157*, 200. (b) Lee, C.; Yang, W.; Parr, G. *Phys. Rev. B* **1988**, *37*, 785.

(16) (a) Haeusermann, U.; Dolg, M.; Stoll, H.; Preuss, H. *Mol. Phys.* **1993**, *78*, 1211. (b) Kuechle, W.; Dolg, M.; Stoll, H.; Preuss, H. *J. Chem. Phys.* **1994**, *100*, 7535. (c) Leininger, T.; Nicklass, A.; Stoll, H.; Dolg, M.; Schwerdtfeger, P. *J. Chem. Phys.* **1996**, *105*, 1052.

(17) (a) McClean, A. D.; Chandler, G. S. *J. Chem. Phys.* **1980**, *72*, 5639. (b) Krishnan, R.; Binkley, J. S.; Seeger, R.; Pople, J. A. *J. Chem. Phys.* **1980**, *72*, 650. (c) Wachters, A. J. H. *J. Chem. Phys.* **1970**, *52*, 1033. (d) Hay, P. J. *J. Chem. Phys.* **1977**, *66*, 4377. (e) Raghavachari, K.; Trucks, G. W. *J. Chem. Phys.* **1989**, *91*, 1062. (f) Binning, R. C.; Curtiss, L. A. *J. Comput. Chem.* **1995**, *103*, 6104. (g) McGrath, M. P.; Radom, L. *J. Chem. Phys.* **1991**, *94*, 511.